

Constraining Evolution of Quintessence with CMB and SNIa Data

Wolung Lee* and Kin-Wang Ng†

*Institute of Physics, Academia Sinica,
Nankang, Taipei, Taiwan 11529, R.O.C.*

(Dated: October 24, 2018)

Abstract

The equation of state of the hypothetical dark energy component, which constitutes about two thirds of the critical density of the universe, may be very different from that of a cosmological constant. Employing a phenomenological model, we investigate semi-analytically the constraints imposed on the scalar quintessence by supernovae observations, and by the acoustic scale extracted from recent CMB data. We show that a universe with a quintessence-dominated phase in the dark age is consistent with the current observational constraints.

PACS numbers: 98.80.Es, 95.35.+d, 98.70.Vc

arXiv:astro-ph/0209093v2 13 Feb 2003

*Electronic address: leewl@phys.sinica.edu.tw

†Electronic address: nkw@phys.sinica.edu.tw

I. INTRODUCTION

Recent astrophysical and cosmological observations such as dynamical mass, Type Ia supernovae (SNe), gravitational lensing, and cosmic microwave background (CMB) anisotropies, concordantly prevail a spatially flat universe containing a mixture of matter and a dominant smooth component, which provides a repulsive force to accelerate the cosmic expansion [1]. The simplest candidate for this invisible component carrying a sufficiently large negative pressure is a true cosmological constant. The current data, however, are consistent with a somewhat broader diversity of such a repulsive “dark energy” as long as its equation of state approaches that of the cosmological constant at recent epoch. A dynamically evolving scalar field ϕ called “quintessence” (Q) is probably the most popular scenario so far to accommodate the dark energy component. It is very interesting and fundamentally important to distinguish the Q field from the true cosmological constant case.

Many efforts have been put forth to reconstruct the scalar potential $V(\phi)$ from observational data based on various reasonable physical motivations. They include pseudo Nambu-Goldstone boson, inverse power law, exponential, tracking characteristics, oscillating feature, and others [2]. Several attempts have been made to test different Q-models [3]. Nevertheless, it proves to be premature at this stage to perform a meaningful data fitting to a particular quintessence model, or to differentiate between the variations. Reconstruction of $V(\phi)$ would likely require next-generation observations.

Since the scalar potential of the Q-field is scarcely known, it is convenient to discuss the evolution of ϕ through its equation of state, $p_\phi = w_\phi \rho_\phi$. Physically, $-1 \leq w_\phi \leq 1$, where the former equality holds for a pure vacuum state. Lately some progress has been made in constraining the behavior of Q field from observational data. A combined large scale structure, SNe, and CMB analysis has set an upper limit on Q models with a constant $w_\phi < -0.7$ [4, 5], and a more recent analysis of CMB observations gives $w_\phi = -0.82^{+0.14}_{-0.11}$ [6]. Furthermore, the SNe data and measurements of the position of the acoustic peaks in the CMB anisotropy spectrum have been used to put a constraint on the present $w_\phi^0 \leq -0.96$ [7]. The apparent brightness of the farthest SN observed to date, SN1997ff at redshift $z \sim 1.7$, is consistent with that expected in the decelerating phase of the flat Λ CDM model with $\Omega_\Lambda \sim 0.7$ [8], inferring $w_\phi = -1$ for $z < 1.7$.

Given the above observational constraints, one would like to know the possible role played by the Q field in the early universe. If the dark energy is a pure cosmological constant or it has a constant equation of state of $\lesssim -0.7$, it would be quickly dominated by the matter for $z > 0.3$. The situation may be very different for quintessence with a time-dependent w_ϕ . Here we will adopt a model-independent approach in which a phenomenological form for the time-dependent w_ϕ is assumed and then used to unfold the dynamics of the Q field up to the epoch of the last scattering surface. In particular, we focus on the CMB constraints that apply to such a generic quintessence (GQ) scenario in the hope of distinguishing the Q field from the true cosmological constant and the constant equation of state.

II. QUINTESSENTIAL COSMOLOGY

Consider a flat universe in which the total density parameter of the universe today is represented by $\Omega_0 = \Omega_m^0 + \Omega_r^0 + \Omega_\phi^0 = 1$ with a negligible Ω_r^0 and $\Omega_m^0/\Omega_\phi^0 \sim 1/2$. Assuming

a spatially homogeneous ϕ field, the evolution of the cosmic background is governed by

$$\frac{d\rho_\phi}{d\eta} = -3a\mathcal{H}(1+w_\phi)\rho_\phi, \quad (1)$$

$$\frac{d\mathcal{H}}{d\eta} = -\frac{3}{2}a\mathcal{H}^2 - \frac{a}{2}(w_r\rho_r + w_\phi\rho_\phi), \quad (2)$$

where the conformal time $\eta = H_0 \int dt a^{-1}(t)$ with the scale factor a and the Hubble constant H_0 , we have used $(d\phi/dt)^2 = (1+w_\phi)\rho_\phi$ and $V(\phi) = (1-w_\phi)\rho_\phi/2$, and rescaled the energy density of the i -th component by the reduced Planck mass $M_p \equiv (8\pi G)^{-1/2}$ and H_0 , i.e. $\rho_i \equiv \rho_i/(M_p H_0)^2$. Accordingly, the dimensionless Hubble parameter is given by

$$\mathcal{H}^2 \equiv \left(\frac{H}{H_0}\right)^2 = \Omega_m^0 a^{-3} + \Omega_r^0 a^{-4} + \Omega_\phi \mathcal{H}^2. \quad (3)$$

Therefore, given a prescribed function of time for the equation of state, $w_\phi(\eta)$, the problem is reduced to solving a set of first-order coupled ordinary differential equations (1) and (2) with the initial conditions set at the present time and the time variable running backwards.

It is well-known that $w_\phi \neq 0$ after last scattering would result in a time-varying Newtonian potential which produces anisotropies at large angular scales through the integrated Sachs-Wolfe effect. If we are to constrain dynamical Q models, it will be useful to define an Ω_ϕ -weighted average [9]

$$\langle w_\phi \rangle = \int_{\eta_{\text{dec}}}^{\eta_0} \Omega_\phi(\eta) w_\phi(\eta) d\eta \times \left(\int_{\eta_{\text{dec}}}^{\eta_0} \Omega_\phi(\eta) d\eta \right)^{-1}, \quad (4)$$

where η_0 and η_{dec} are respectively the conformal time today and at the last scattering. It was shown [5, 9] that as far as the CMB anisotropy power spectrum is concerned, the time-averaged $\langle w_\phi \rangle$ is well approximated by an effective constant w_ϕ for models in which the Q component is negligible at the last scattering.

III. THE GENERIC QUINTESSENCE SCENARIO

The generic quintessence scenario assumes a phenomenological form for the equation of state w_ϕ to accommodate as many observational outcomes as possible. Here we take $\Omega_m^0 = 0.3$ and $\Omega_r^0 = 9.89 \times 10^{-5}$ with $w_r = 1/3$. Note that $\Omega_\phi^0 = 1 - \Omega_m^0 - \Omega_r^0 \simeq 0.7$. Let us start with the form for w_ϕ at low redshifts. In order to satisfy the above-mentioned SNe observational constraints on w_ϕ , we are bound to choose $w_\phi = -1$ for $z \lesssim 2$. As such, the quintessence behaves just like a cosmological constant for $0 < z < 2$, and it becomes dominated by the matter density at $z \sim 0.3$. This can be seen in an example of the GQ in Fig. 1. We have also plotted $d\theta/d\eta = a\sqrt{(1+w_\phi)\rho_\phi}$, where $\theta \equiv \phi/M_p$. For the Q field to obtain maximal dynamics at low redshifts, w_ϕ has to increase abruptly to unity for $z > 2$. However, if w_ϕ remains at unity for too long, it would induce an unacceptably large integrated Sachs-Wolfe effect on the CMB large-scale anisotropy. In Fig. 1, we have chosen a width of the square-wave form of w_ϕ such that $\langle w_\phi \rangle \simeq -0.7$, which saturates the above-mentioned upper limit from CMB data on a constant w_ϕ [4]. We thus see that Ω_ϕ can reach a value of 0.42 at $z \sim 23$ at which w_ϕ is forced to decrease to a negative value. On the other hand, a Q component with a constant $w_\phi = -0.7$ is dominated by matter for

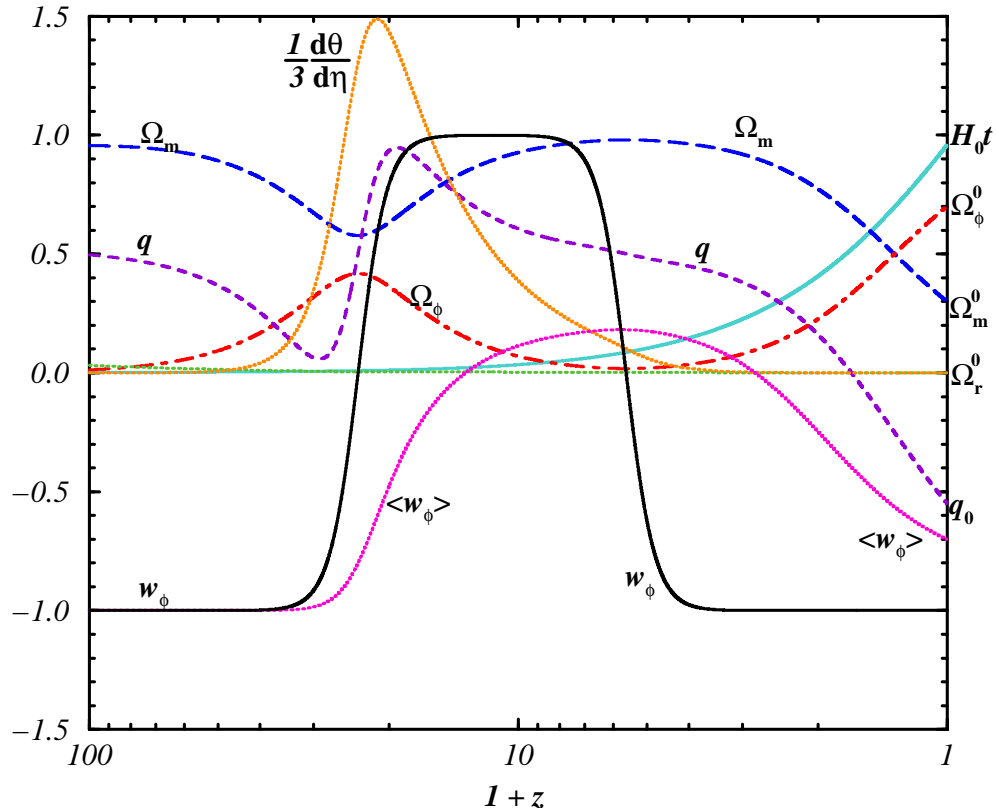


FIG. 1: An example of GQ scenario

$z > 0.5$. Also note that at the present time $H_0 t = 0.95$, and we have plotted the history of the deceleration parameter q .

The above GQ model exemplifies an extreme case on how the quintessence may be different from a cosmological constant for $z > 2$. If we shift the square-wave of w_ϕ to higher redshifts while keeping $\langle w_\phi \rangle \simeq -0.7$, the integrated Sachs-Wolfe effect on the CMB anisotropy power spectrum would be almost the same. Meanwhile, the dynamics of the Q field will take place at higher redshifts accordingly. This will be valid until the Q component becomes significant at the last scattering.

IV. CMB ACOUSTIC PEAKS AND QUINTESSENCE

We now turn to study the effect of the presence of the Q component at the time of last scattering on the CMB acoustic peaks. The tightly coupled baryon-photon plasma experienced a serial acoustic oscillation just before the recombination epoch. The acoustic scale (the angular momentum scale of the acoustic oscillation) sets the locations of the peaks

in the power spectrum of the CMB anisotropies [10], and is characterized by

$$l_A = \pi \frac{d_*}{h_s} = \pi \frac{\eta_0 - \eta_{\text{dec}}}{\int_0^{\eta_{\text{dec}}} c_s d\eta}, \quad (5)$$

where d_* represents the comoving distance to the last scattering surface and h_s denotes the sound horizon at the decoupling epoch with the sound speed c_s . Both d_* and h_s are affected in the presence of the Q component. Furthermore, the location of the m -th peak can be parametrized in practice by the empirical fitting formula, $l_m = l_A(m - \varphi_m)$, where the phase shift φ_m caused by the plasma driving effect is solely determined by pre-recombination physics [11]. It was shown [12] that the shift of the third peak is relatively insensitive to cosmological parameters. Consequently, by assuming $\varphi_3 = 0.341$, the value of the acoustic scale derived from the analysis of BOOMERANG data [13] lies in the range [14]

$$l_A = 316 \pm 8, \quad (6)$$

which is estimated to be within one percent error if the location l_3 is measured.

To impose the constraint from the peak separation of CMB, one needs to calculate the acoustic scale l_A in Eq. (5) for different GQ models. Since the sound speed in the pre-recombination plasma is characterized by [10]

$$c_s = \frac{1}{\sqrt{3(1+R)}} \quad \text{with} \\ R \equiv \frac{3\rho_b}{4\rho_\gamma} \approx 30230 \left(\frac{T_\gamma^0}{2.728K} \right)^{-4} \frac{\Omega_b^0 h^2}{1+z}, \quad (7)$$

where $H_0 = 100 h \text{kms}^{-1} \text{Mpc}^{-1}$ and the baryon-photon momentum density ratio R sets the baryon loading to the acoustic oscillation of CMB, the sound horizon h_s at the decoupling epoch can be determined by the differential equation

$$\frac{dh_s}{d\eta} = c_s, \quad (8)$$

coupled with the background evolution equations (1) and (2). Using $\Omega_b^0 = 0.05$, $h = 0.65$, and fixing the last scattering surface at $z_{\text{dec}} = 1100$, we have calculated the acoustic scales of different GQ models by shifting the square-wave of w_ϕ towards the last scattering surface while keeping $\langle w_\phi \rangle$ a constant. Figure 2 plots the results against the Q energy density at decoupling $\Omega_\phi(z_{\text{dec}})$ with contours $\langle w_\phi \rangle = -0.5, -0.6, -0.7, -0.8, -0.9$, and -1 . The last one is simply the Λ CDM model. In general, when $\langle w_\phi \rangle$ is fixed, the acoustic scale is proportional to the quintessence density at the last scattering surface. On the other hand, for a fixed $\Omega_\phi(z_{\text{dec}})$, the acoustic scale decreases as $\langle w_\phi \rangle$ increases. The two horizontal lines are drawn as the upper- and lower-bounds of the acoustic scale derived from the BOOMERANG data (6). All GQ models lying in the region above the curve of $\langle w_\phi \rangle = -0.7$ and within the BOOMERANG bounds are consistent with the current CMB data. Thus, the model depicted in Fig. 1 is disfavored as far as the acoustic peak location is concerned. We have presented an extreme model located at the upper right corner of the allowed region in Fig. 3, i.e. $(\langle w_\phi \rangle, \Omega_\phi^{\text{dec}}) = (-0.7, 0.59)$. The figure shows the detailed background evolution of the model, in which the Q component dominates over the matter density for $1380 > z > 130$ and the deceleration parameter q is negative for $1400 > z > 430$.

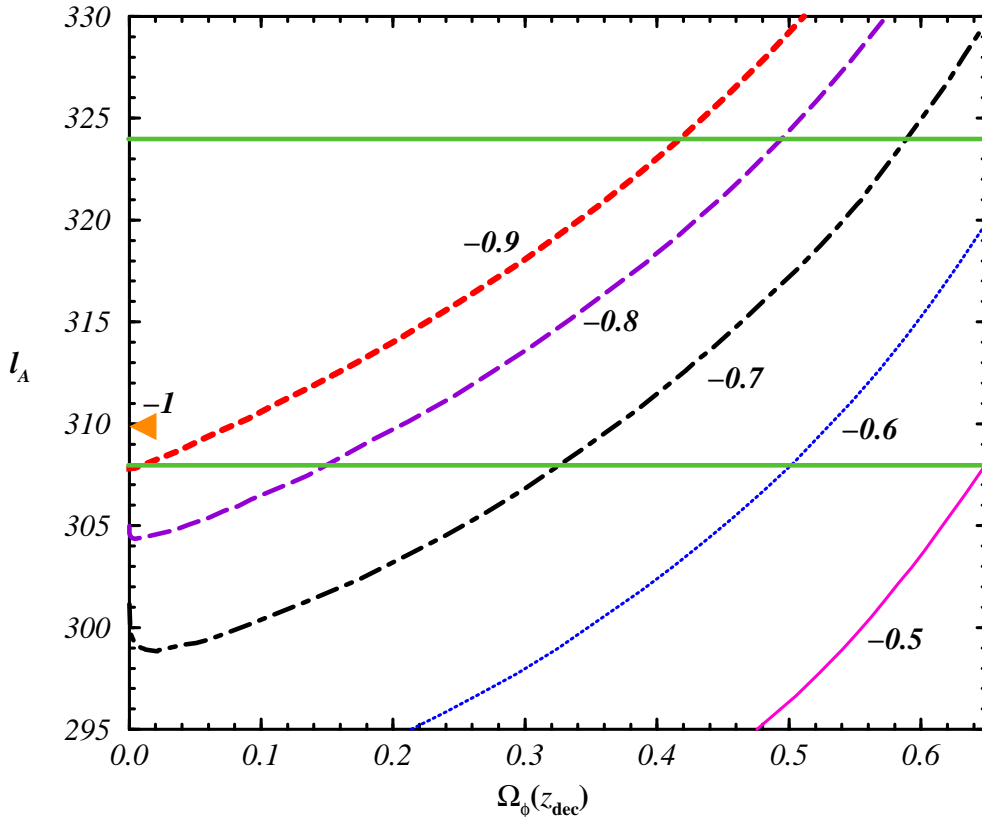


FIG. 2: Acoustic scales of the GQ models are plotted as a function of the quintessence density at decoupling while keeping the Ω_ϕ -weighted averaged equation of state fixed. The model equivalent to the cosmological constant case has $l_A \simeq 310$ and is denoted by a solid triangle. The two horizontal lines signify the upper- and lower-bounds permitted by the BOOMERANG data.

V. THE AMPLITUDE OF MATTER POWER SPECTRUM

It is well known that a non-zero Ω_ϕ would lead to a suppression of the growth of matter perturbations. It is therefore useful to study the constraint from the growth of structure on the GQ model. Let us consider the growth function for matter perturbations on scales smaller than the smoothing scale of the quintessence governed by the differential equation,

$$\frac{d^2\delta}{d\eta^2} + a\mathcal{H}\frac{d\delta}{d\eta} - \frac{3}{2}a^2\mathcal{H}^2\Omega_m\delta = 0. \quad (9)$$

We have evaluated the growth function $\delta(\eta)$ for the extreme GQ model in Fig. 3. Compared to the Λ CDM model, the growth of δ from the radiation-matter equality to $\eta = \eta_0$ is suppressed by about a factor of 2 (see Fig. 5). When normalized to the COBE data, the resulting CMB anisotropy power spectrum has a significant excess of power at $l \sim 100$. In order to keep the suppression of the growth function stable at about 30% level, we have found that $\langle w_\phi \rangle$ has to be less than about -0.9 in Fig. 2. An accurate determination

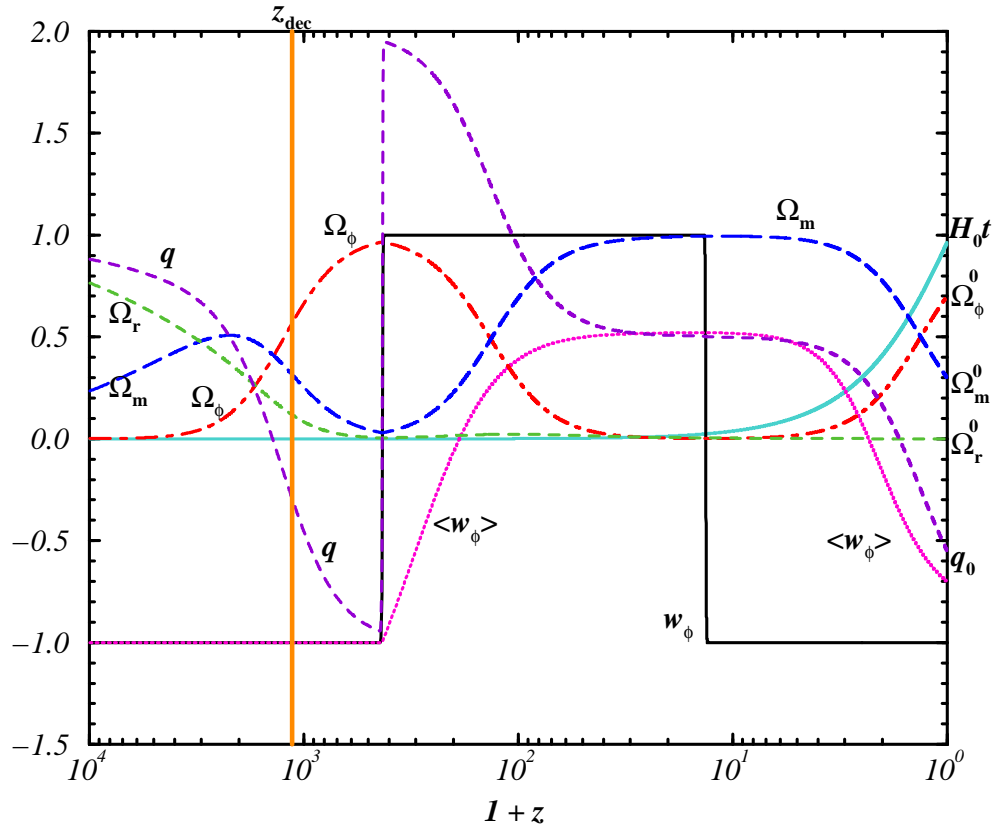


FIG. 3: Background evolution of an extreme GQ model with $(\langle w_\phi \rangle, \Omega_\phi^{\text{dec}}) = (-0.7, 0.59)$. The last scattering surface is marked as the vertical line at $z_{\text{dec}} = 1100$.

would require computing small-scale matter perturbations as well as performing a maximum-likelihood fitting to the existing CMB anisotropy data. We have plotted in Fig. 4 an extreme model located at the upper end of the contour $\langle w_\phi \rangle = -0.9$ where $\Omega_\phi^{\text{dec}} = 0.42$, and the growth function of this model in Fig. 5. In this case, the Q component dominates over the matter density for $1100 > z > 590$ and the deceleration parameter q is negative for $1150 > z > 810$.

VI. CONCLUSION AND DISCUSSION

We have investigated the evolution of the quintessence allowed by the observational constraints from CMB and SNe, using a semi-analytic method with a simple square-wave function for the time-varying equation of state. Although the true equation of state, if there is any, may be a complicated function of time, the square-wave should roughly capture the generic feature of the evolution of the quintessence. This generic quintessence model is sufficient for us to confront the current observational data. Future high-precision data will tighten the constraints to this model and we may even need a more sophisticated model to parametrize the physics of the Q component. Also, the present method gives more physical

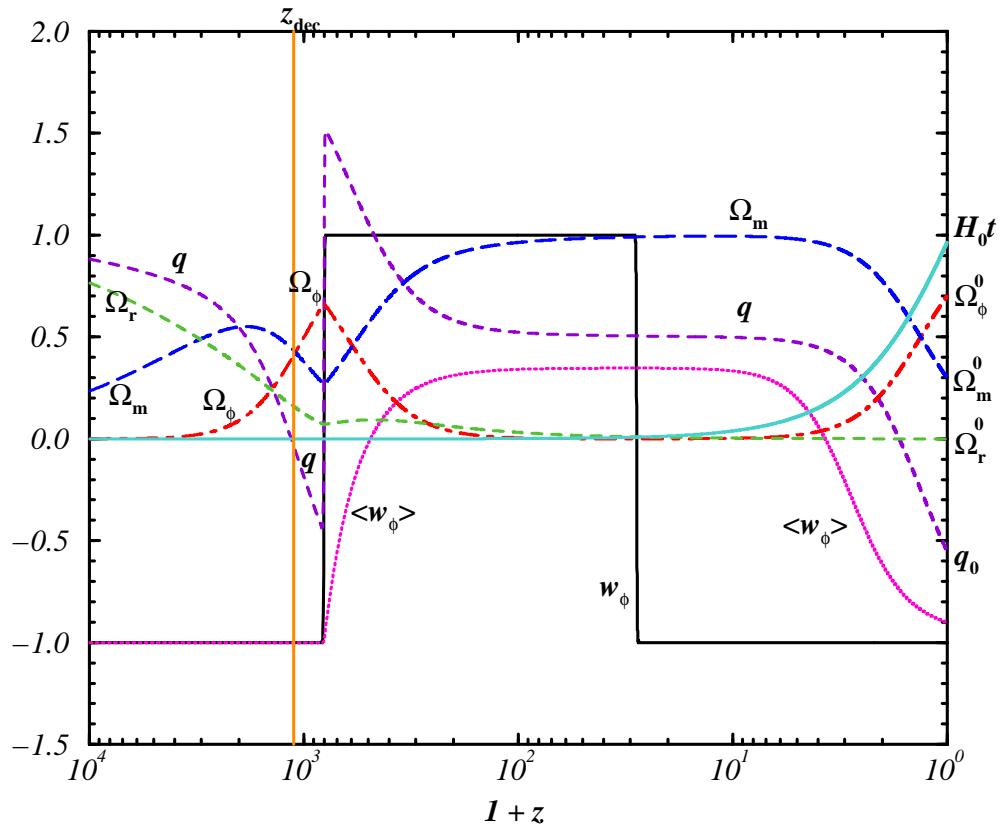


FIG. 4: Background evolution of an extreme GQ model with $(\langle w_\phi \rangle, \Omega_\phi^{\text{dec}}) = (-0.9, 0.42)$.

insights and is much simpler though less accurate than the numerically intensive maximum likelihood analysis of CMB data (see, e.g., Ref. [15]).

Three extreme GQ models have been presented. Figure 1 shows the maximum dynamics that the Q field can attain at low redshifts for $z > 2$. The evolving Q field during the large-scale-structure formation may have interesting cosmological implications. For instance, the authors in Ref. [16] have attempted to generate primordial magnetic fields from the dynamics of the Q field coupled to electromagnetism. This electromagnetic Q field may also be responsible for the time-varying fine structure constant (α) [17] as it was recently claimed that the results of a search for time variability of α using absorption systems in the spectra of distant quasars yield a smaller α in the past [18]. We have also studied the constraint from the growth of large-scale matter perturbations on the GQ model. Figure 4 shows that the Q component can make up about 40% of the total energy density of the universe at last scattering. This result is consistent with the upper bound $\Omega_\phi < 0.39$ during the radiation dominated epoch obtained by performing a maximum likelihood analysis on the CMB data [15]. In general, the GQ scenario bears a salient feature that the Q component overwhelms the matter during the dark age. It is worth studying in more details about its influence on the evolution of matter perturbations and the subsequent structure formation. At last, we would like to point out that an acceleration of the universe in the past is consistent

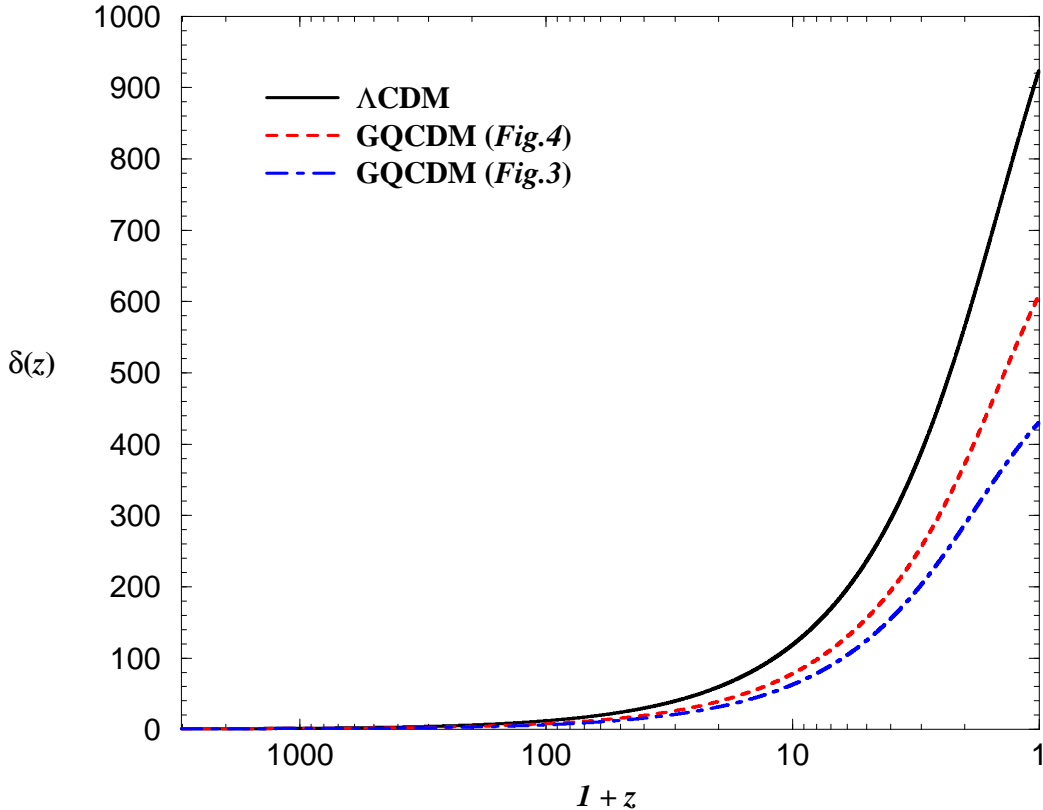


FIG. 5: Growth functions of large-scale matter perturbations with unity normalization at radiation-matter equality time for the Λ CDM model and the GQ models in Fig. 3 and Fig. 4.

with all observations. So the fact that the universe is accelerating today would not be quite unnatural.

Acknowledgments

This work was supported in part by the National Science Council, Taiwan, ROC under the Grant NSC91-2112-M-001-026.

-
- [1] See, e.g., L. Wang, R. R. Caldwell, J. P. Ostriker, and P. J. Steinhardt, *Astrophys. J.* **530**, 17 (2000).
[2] I. Waga and J. A. Frieman, *Phys. Rev. D* **62**, 043521 (2000); S. Dodelson, M. Kaplinghat, and E. Stewart, *Phys. Rev. Lett.* **85**, 5276 (2000); C. Skordis and A. Albrecht, *Phys. Rev. D* **66**, 043523 (2002); L. A. Boyle, R. R. Caldwell, M. Kamionkowski, *Phys. Lett. B* **545**, 17 (2002); T. Chiba, *Phys. Rev. D* **64**, 103503 (2001); and references therein.

- [3] P. Brax, J. Martin, and A. Riazuelo, *Phys. Rev. D* **62**, 103505 (2000); C. Baccigalupi, S. Matarrese, and F. Perrotta, *Phys. Rev. D* **62**, 123510 (2000); A. Balbi *et al.*, *Astrophys. J.* **547**, L89 (2001); L. Amendola, *Phys. Rev. Lett.* **86**, 196 (2001); M. Pavlov, C. Rubano, M. Sazhin, and P. Scudellaro, *Astrophys. J.* **566**, 619 (2002); B. F. Roukema, G. A. Mamon, and S. Bajtlik, *Astron. Astrophys.* **382**, 397 (2002); M. Yahiro *et al.*, *Phys. Rev. D* **65**, 063502 (2002).
- [4] J. R. Bond *et al.*, in *Proceedings of Verbier 2000, Cosmology and Particle Physics*, astro-ph/0011379.
- [5] R. Bean and A. Melchiorri, *Phys. Rev. D* **65**, 041302(R) (2002).
- [6] C. Baccigalupi *et al.*, *Phys. Rev. D* **65**, 063520 (2002).
- [7] P. S. Corasaniti and E. J. Copeland, *Phys. Rev. D* **65**, 043004 (2002).
- [8] A. G. Riess *et al.*, *Astrophys. J.* **560**, 49 (2001); M. S. Turner and A. G. Riess, astro-ph/0106051; N. Benitez *et al.*, *Astrophys. J.* **577**, L1 (2002).
- [9] G. Huey *et al.*, *Phys. Rev. D* **59**, 063005 (1999).
- [10] W. Hu and N. Sugiyama, *Astrophys. J.* **444**, 489 (1995).
- [11] W. Hu, M. Fukugita, M. Zaldarriaga, and M. Tegmark, *Astrophys. J.* **549**, 669 (2001).
- [12] M. Doran and M. Lilley, *Mon. Not. R. Astron. Soc.* **330**, 965 (2001).
- [13] P. de Bernardis *et al.*, *Astrophys. J.* **564**, 559 (2002).
- [14] M. Doran, M. Lilley, and C. Wetterich, *Phys. Lett. B* **528**, 175 (2002).
- [15] R. Bean, S. H. Hansen, and A. Melchiorri, *Phys. Rev. D* **64**, 103508 (2001).
- [16] D.-S. Lee, W.-L. Lee, and K.-W. Ng, *Phys. Lett. B* **542**, 1 (2002).
- [17] G. Dvali and M. Zaldarriaga, *Phys. Rev. Lett.* **88**, 091303 (2002); T. Chiba and K. Kohri, *Prog. Theor. Phys.* **107**, 631 (2002); K.-W. Ng, in *Proceedings of the First NCTS Workshop on Astroparticle Physics*, edited by H. Athar *et al.* (World Scientific, Singapore, 2002).
- [18] J. K. Webb *et al.*, *Phys. Rev. Lett.* **87**, 091301 (2001).